JOURNAL OF MATERIAL SCIENCE 30 (1995) 3704–3710

Interface reactions between $YBa_2Cu_3O_{7-x}$ and W, Si or WSi_2

R. BOHNENKAMP-WEIß, R. SCHMID-FETZER*
Technische Universität Clausthal, AG Elektronische Materialien, Robert-Koch-Str. 42, D-38678 Clausthal-Zellerfeld, Germany

The chemical compatibility between $YBa_2Cu_3O_{7-x}$ (Y123) and W, Si or WSi_2 was studied using quasi-infinite diffusion couples which were encapsulated and annealed at 650 to 800 °C for 5–80 h. The phases formed at the interface and the morphology and growth kinetics of the reaction zone were analysed in cross-sections of these couples using optical and scanning electron microscopy together with energy- and wavelength dispersive X-ray microanalysis. A Si/Y123 sample was also studied using secondary ion mass spectroscopy (SIMS). In addition, bulk powder mixtures of Y123 with W, Si or WSi_2 were equilibrated at 800 °C for 100–300 h and phase analysis was performed using X-ray diffraction.

The following primary reactions are identified, for tungsten: $6YBa_2Cu_3O_7 + 7W \rightarrow 2BaWO_4 + 5Ba_2WO_5 + 3Y_2O_3 + 18Cu$ and for silicon: $2YBa_2Cu_3O_{6.5} + 3Si \rightarrow 2BaSiO_3 + Ba_2SiO_4 + Y_2O_3 + 6Cu$. The reactivity of WSi_2 is not much smaller compared to that of elemental W and Si. The results of diffusion couples and bulk samples are consistent and complement each other, the dominant product phases are observed in both experiments. A diffusion controlled mechanism with a parabolic growth law and a relatively small activation energy ($Q = 44\ kJ\ mol^{-1}$) is verified for the W/Y123 reaction. In both the W/Y123 and Si/Y123 couples the dominantly diffusing species are barium and oxygen. Barium diffuses far through the reaction zone to form double oxides, leaving a fine grained Y–Cu–O layer behind (mostly Y_2O_3 + Cu), and eventually the entire superconductor phase Y123, being depleted of Ba, turns into this Y–Cu–O mixture.

1. Introduction

Chemical reactions at the interface between $YBa_2Cu_3O_{7-x}$ (Y123) and other materials like tungsten or silicon have a strong impact on the technological application of this high temperature superconductor in multilayer materials. They are also important in shape forming processes with mixtures of these materials and for the development of diffusion barriers. In all of these applications the material combination is usually subject to a high temperature annealing, which is also aimed at producing the proper oxygen stoichiometry.

Interface reactions between Y123 ceramic and thin Si films occurring up to 300 °C were studied using auger electron spectroscopy (AES) and disappearance potential spectroscopy (DAPS) [1]. At room temperature the formation of a thin SiO_2 interlayer is observed, which prevents further withdrawal of oxygen from the superconductor, confirming earlier data [2, 3]. However, upon annealing above 100 °C the entire Si film (3 nm) becomes oxidized and above 200 °C an enrichment of Ba, which diffuses to the top of the film, was observed [1].

Reactions in powder mixtures of Y123 with Si, WC, CaF_2, SiO_2 and other oxide materials at 600–900 °C were studied using X-ray diffraction (XRD) and susceptibility measurements. Both Si and SiO_2 react with Y123 and the formation of Ba_2SiO_4 was reported [4]. In the W–Y–Ba–Cu–O system a superconducting compound $Ba_2YCu_2WO_y$ ($T_c = 77$ K) was discovered [5, 6].

The diffusion of elemental species in Y123 was studied using radioactive tracers and the diffusion coefficients were found to decrease in the sequence (O > Cu > Ba ≈ Y) at temperatures of 850–980 °C [7]. However, for a theoretical description of the pertinent reaction diffusion with formation of new phases at the interface, the diffusion coefficients of all species in each of these phases would be needed, and these data are not available.

One needs to know more about reactions at the interface from an experimental approach in order to optimize annealing treatments. These data are also important for the selection of appropriate metals or intermetallic phases as contact materials to Y123 or as intermediate layers and also for an understanding of adhesion mechanisms after annealing.

* Author to whom correspondance should be addressed.

0022–2461

The purpose of this study is to investigate the reaction diffusion in quasi-infinite diffusion couples, which enables the long-term observation of reactions and to correlate these findings with the phase formation in equilibrated powder mixtures. The focus is on the following questions: (i) which new phases are formed at the interface, (ii) what is the morphology and growth kinetics of the reaction zone, and (iii) what are the approximate thermodynamic driving forces that may be estimated for these complex reactions?

2. Experimental procedure

2.1. Materials and preparation

The superconductor Y123 was prepared by ceramic processing. Y_2O_3, CuO and $BaCO_3$ powder was mixed in a 1:2:3 ratio of metal atoms and milled for 1 h in an agate mortar. The powder was lightly compacted, annealed for 48 h in air at 925 °C, crushed, milled again and pressed in a die at 30 kN into a tablet of 8 mm diameter. After a second sintering at 925 °C for 48 h in air the sample was slowly (0.8 °C min^{-1}) cooled to obtain the correct stoichiometry $YBa_2Cu_3O_{6.8}$, which was checked using thermogravimetric analysis and iodometric titration; the density of the Y123 tablet was 75–80% of theoretical.

The existence of the pure orthorhombic $YBa_2Cu_3O_{6.8}$ with no foreign phase was confirmed by XRD, the spectrum was identical to the one given by Woong-Ng and co-workers [8]. The superconductivity was routinely checked using the Meissner-effect. For one specimen the critical temperature (T_c = 86 K) was determined from resistivity measurements.

Data on the commercially obtained materials are given in Table I which also gives a summary of subsequent processes.

2.2. Diffusion couples

Diffusion couples were prepared as a sandwich from a Y123 tablet covered on both sides with W foil or, in separate experiments, with Si wafer. This sandwich was protected on both sides with Al_2O_3 discs and placed in a capsule machined from copper or stainless steel as shown in Fig. 1. A screw-in lid was used to apply the same initial pressure to all diffusion couples.

TABLE I Materials and processes

Material	Purity (mass %)	Process
Y_2O_3	99.99%	Y123 tablets: grinding,pressing
CuO	99.9%	925 °C/48 h (twice)
$BaCO_3$	99.9%	Y123 powder: ground tablets
W foil 0.5 mm	99.98%	diffusion couples: W/Y123, Si/Y123
Si wafer 1 mm	> 99.999%	650–800 °C/ 5–80 h
W wire ϕ = 0.25 mm	99.98%	bulk samples
W powder 100 mesh	99.98%	W, Si, WSi_2 + Y123 powder
Si powder 100 mesh	99.9%	800 °C/ 100–300 h
WSi_2 powder 200 mesh	99.9%	

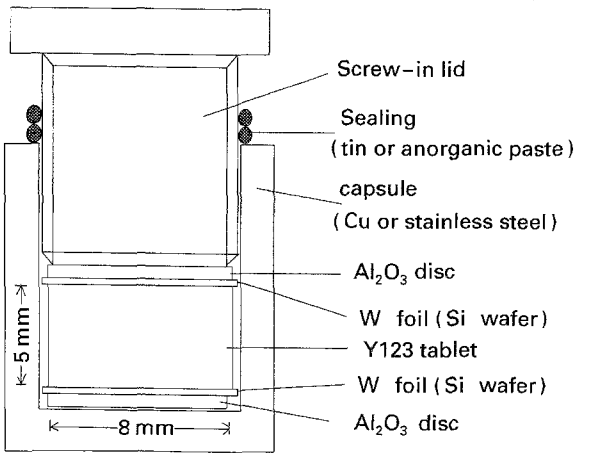

Figure 1 Schematic diagram of the mounting of the diffusion couple in the capsule.

The Cu capsules were sealed with a tin wire, which alloys during heating. For the steel capsules, used above 700 °C, a gas-tight anorganic paste (Thermoguss 2000) was applied. The purpose of the sealing was to prevent an oxygen out-diffusion from the capsule into the furnace atmosphere (flowing argon, 99.998% Ar) or vice versa. The sealing was tested to be efficient enough to prevent the oxidation of a thin graphite wire in an empty capsule.

The capsules were placed in the preheated furnace at constant temperature (650–800 °C), annealed for 5, 20 or 80 h and quenched in water. A cross-section of the sample was carefully cut using a low speed diamond saw. The metallographic preparation of the cross-section was complicated in view of the very different materials and phases. Best results were obtained by lapping with a diamond suspension (9 μm) and subsequent polishing first using a silk and then a wool cloth with diamond paste down to 1 μm. More details are given by Bohnenkamp-Weiß [9].

The cross-sections were analysed using optical microscopy with quantitative image analysis. In addition, scanning electron microscopy with energy dispersive X-ray analysis (SEM/EDX) and an electron microprobe with wavelength dispersive X-ray analysis (WDX) was used for line scan and spot analysis of chemical composition. A Si/Y123 sample was also studied using secondary ion mass spectroscopy (SIMS).

The WSi_2/Y123 couple was prepared differently since a WSi_2 foil was not available. A smaller Y123 tablet (5 mm diameter) was completely embedded in WSi_2 powder and pressed to a tablet of 8 mm diameter. This tablet was annealed in an evacuated silica capsule at 800 °C for 100 h. Since a cross-section of this tablet could not be prepared, phase analysis was done using XRD only and, on the reacted core, SEM/EDX.

2.3. Bulk samples

Bulk samples were prepared from powder mixtures of Y123 with W, Si or WSi_2 since they can provide an insight to the equilibrium state after complete reaction because of the much larger contact area. The Y123 powder was obtained by grinding the Y123 tablets described in Section 2.1. It was mixed with W or Si powder and also, for comparison, with granular material (cut W wire or crushed Si wafer). These mixtures, with a total mass of 1–2 g and 67–94 mass% Y123, were pressed gently by hand in a die and sealed in evacuated silica capsules. After annealing at 800 °C for more than 100 h the capsules were quenched in water. The annealing time required for equilibration was determined in preliminary experiments. No sticking of the specimen to the silica capsule was observed, indicating no major side reactions with the container. The samples were pulverized and phase analysis was performed using XRD.

3. Results and discussion

3.1. Tungsten

3.1.1. Diffusion couples W/Y123

A typical reaction zone between W and Y123 is shown in Fig. 2. The reaction starts at 650 °C/1 h with the formation of tungsten oxide (WO_z). Upon more intensive annealing the reaction proceeds with the formation of a multilayer reaction zone $WO_z/BaWO_4/Ba_2CuWO_6$/Y–Cu–O which grows as given in Table II. The statistical accuracy of the thickness, measured at various locations of the section, is about ± 4 μm, mainly because of the rough interfaces visible in Fig. 2.

The composition of the WO_z zone varies from $WO_{2.5}$ to WO_3 in the direction towards Y123, as measured by a comparison of the W-intensities in EDX analysis. This is possibly a sequence of the oxides $WO_{2.72} \rightarrow WO_{2.9} \rightarrow WO_3$. This WO_z zone grows with increasing temperature but remains virtually constant between 5 and 80 h at fixed temperatures.

A Y–Cu–O layer forms adjacent to the residual Y123 with a wavy interface. This layer becomes very broad with increasing temperature. Its fine grain structure, less than 2 μm, can only be resolved by optical microscopy and not by backscattering images in the SEM. This impeded a more precise analysis, however, the Ba and W content is definitely below the detection limit of EDX. The Y–Cu–O layer may possibly consist of Y_2O_3 and Cu.

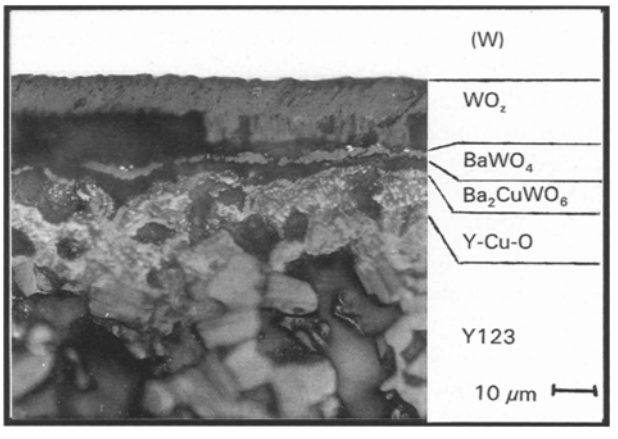

Figure 2 Cross-sectioned reaction zone of a W/Y123 sample after 20 h at 700 °C (optical micrograph).

TABLE II Growth of reaction zone R with total thickness d at various annealing temperatures and times in quasi-infinite W/R/Y123 diffusion couples

	5 h		20 h		80 h	
T [°C]	R	d (μm)	R	d (μm)	R	d (μm)
650	WO_z	18	M	28	M	40
700[a]	M	25	M	30	M	32
750	M	22	M	45	M	50
800	M	45	M	75	M	90

[a] Possible side reactions with Cu capsule at 700 °C.
M = multiphase zone $WO_z/BaWO_4/Ba_2CuWO_6$/Y–Cu–O.

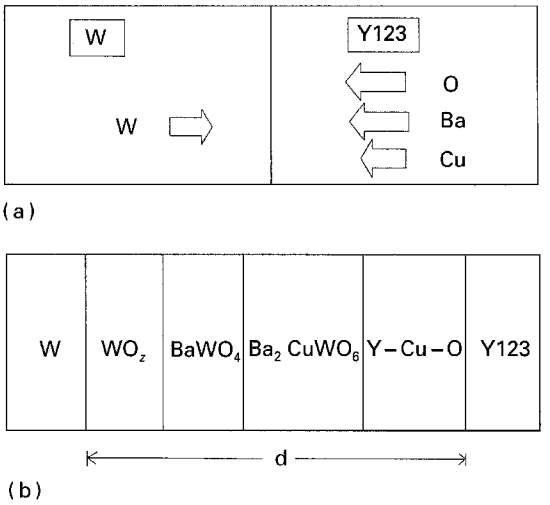

Figure 3 Schematic diagram of a cross-sectioned W/Y123 couple: (a) major species, diffusing through reaction zone; (b) growing phase sequence in the reaction zone R.

The elemental species dominating the diffusion through the reaction zone may be deduced from the sequence of phase layers and their relative growth as depicted schematically in Fig. 3. Oxygen and barium diffuse far through the multilayer zone, forming WO_z and the Ba compounds. In the opposite direction W is also involved in the reaction diffusion and is found in three of the layers. Some copper diffuses at least through the Y–Cu–O layer to form Ba_2CuWO_6. Yttrium may not have to diffuse substantially since the Y–Cu–O layer probably grows mainly by a shift of the Y–Cu–O/Y123 phase boundary and consumption of Y123.

The quantitative growth kinetics of the total reaction zone thickness, d, follows a parabolic law, $d = kt^{1/2}$. This indicates a diffusion-controlled overall growth mechanism. The Arrhenius plot of the growth constant, k, as a function of the absolute temperature, T, is given in Fig. 4. The activation energy is relatively small, $Q = 44\ \mathrm{kJ\,mol^{-1}}$. The irregular data at 700 °C have not been used in this evaluation since they are probably falsified by side reactions with the copper capsule. Oxidation reactions between the superconductor and the Cu wall via the gas phase have

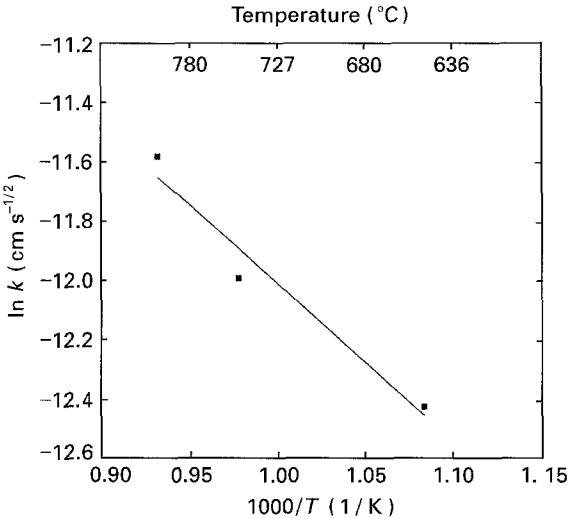

Figure 4 Arrhenius plot of layer growth kinetics in W/Y123 diffusion couples. $d = k^* t^{1/2}$. $\ln k = -Q/R^*T + C$, $Q = 44\,\text{kJ mol}^{-1} = 0.46\,\text{eV}$, $C = -6.72$.

seemingly occurred. At 750 °C and higher temperatures only stainless steel capsules have been used and no side reaction was visible.

3.1.2. Bulk samples Y123+W

The phases identified by XRD in bulk powder mixtures annealed at 800 °C are given in Table III. The structural information used for phase identification is compiled in Table IV. It is remarkable that the Y123 phase was completely reacted in all the samples, even at the highest Y123:W mass ratio of 10:1. An incomplete reaction is to be noted for the first sample, since cut W wire was used instead of W powder. Between the first annealing (100 h) and the second annealing (100 h) additional phases appeared. All of the phases, corresponding to the total annealing time of 200 h, are given in Table III and they are identical to those found in another sample with W wire annealed for 300 h. These W wire samples still do not constitute the equilibrium state as compared to the powder sample of the same overall composition, which was already equilibrated after 100 h with no reaction progress in additional annealings. All the other samples were prepared from W powder and it should be noted that the (W) phase entirely disappeared, except for a faint trace at the higher W content.

As a simplified primary reaction, disregarding mutual solubilities, one may assume

$$6YBa_2Cu_3O_7 + 7W \rightarrow 2BaWO_4 + 5Ba_2WO_5 + 3Y_2O_3 + 18Cu \quad (1)$$

This reaction is also likely compared to other potential reaction products in view of its Gibbs energy of reaction,

$$\Delta G_{(1)}(1100\,\text{K}) \approx -4722.3\,\text{kJ mol}^{-1} = -55.6\,\text{kJ g-atom}^{-1} \quad (2)$$

based on the data given in Barin [10]. The standard states and Gibbs energies of formation are detailed in Table V.

TABLE III Results of bulk samples (Y123 + W) annealed at 800 °C for 100–300 h

Mass ratio (Y123:W)	Phases identified (sequence according to X-ray intensities)
10:1[a]	$W + WO_3 + BaWO_4 + Ba_2Y_{0.667}WO_6$
10:1	$Ba_2Y_{0.667}WO_6 + Y_2BaCuO_5 + Cu_2O + CuO$
4:1	$BaWO_4 + Ba_2WO_5 + Y_2O_3 + Ba_2Y_{0.667}WO_6 + Cu_2O + Cu$
3.09:1	$BaWO_4 + Ba_2WO_5 + Y_2O_3 + Cu$
2:1	$BaWO_4 + Ba_2WO_5 + Y_2O_3 + Cu + W$

[a] W wire used instead of W powder, incomplete reaction.

TABLE IV Crystal structure of relevant phases ([12], JCPDS-file)

Phase	Pearson symbol	Space group	JCPDS card no.
BaO	cF8	$Fm\bar{3}m$	22-1056
CuO	mC8	C2/c	5-0661
Cu_2O	cP6	$Pn\bar{3}m$	5-0667
SiO_2	hP9	$P3_2$-21	33-1161
WO_3	oP16	Pnma	32-1394
WSi_2	tI6	I4/mmm	11-195
Y_2O_3	cI80	$Ia\bar{3}$	25–1200
Ba_2CuO_3	oI48	Immm	39-1497
$BaSiO_3$	oP4	Pmmm	26-1402
Ba_2SiO_4	oP4	Pnam	26-1403
$BaWO_4$	tI4	C^6_{4H}	8-457
Ba_2WO_5	oP4	Pnam	25-1211A
BaY_2O_4	ortho.	Pnab	27-44
$YCuO_2$	hP2	$P6_3/mmc$	39-244
$Y_2Cu_2O_5$	oP4	$Pna2_1$	33-511
Ba_2CuWO_6	tP40	P4/*	38-1378
$Ba_2Y_{0.667}WO_6$	cubic		38-219
$YBa_2Cu_3O_{6.8}$	oP12.8	Pmmm	39-486
Y_2BaCuO_5	oP36	Pbn*3	38-1434

TABLE V Gibbs energy of formation of relevant phases, $\Delta_f G$, from stable elements at 1100 K

Phase	$\Delta_f G$ (1100 K) (kJ mol^{-1})	Ref.
BaO	−447.9	[10]
CuO	−58.0	[10]
WO_3	−561.4	[10]
WSi_2	−85.5	[10]
Y_2O_3	−1586.5	[10]
$BaSiO_3$	−1317.5	[10]
Ba_2SiO_4	−1871.4	[10]
$BaWO_4$	−1326.9	[10]
Ba_2WO_5	−1800	[a]
$YBa_2Cu_3O_{6.7}$	−1948.5[b]	[11]

[a] Estimated from minimum of stability in the BaO–WO_3 system.
[b] Calculated from the value of [11], −85.4 kJ mol^{-1}, referring to the formation from single oxides.

The sample prepared in the stoichiometric proportions of Equation 1 is given with the mass ratio (3.09:1) in Table III and its reaction products are in complete agreement with Equation 1. In fact, the sample with higher W content (2:1) contains some residual W and the sample with lower W content (4:1) contained other additional phases. This also confirms the primary reaction mechanism of Equation 1.

3.2. Silicon

3.2.1. Diffusion couples Si/Y123

A typical cross-section of a Si/Y123 couple reacted at 800 °C is given in Fig. 5. It displays a gap between the residual Si and the reaction layer which is probably due to a poor contact because of the lacking flexibility of the monocrystalline Si wafer, as compared to the W foil. However, the formation or broadening of this gap as an artefact during preparation might also be possible. The formation of a reaction zone is only visible after prolonged annealing, as compiled in Table VI. The kinetics of the layer thickness growth will not be interpreted quantitatively in view of the gap formation.

The reaction zone comprises two layers: a barium silicate which was mostly $BaSiO_3$ with occasional Ba_2SiO_4 and a fine-grained Y–Cu–O layer. This second layer exhibits strongly fluctuating Y/Cu-ratios in the EDX and is probably multiphase (Y_2O_3, Cu, Cu_2O).

A schematic sketch of the major diffusing species is presented in Fig. 6. Barium and oxygen diffuse through the Y–Cu–O layer to form the $BaSiO_3$ (+ Ba_2SiO_4) layer. Silicon may not have to diffuse substantially if this barium silicate layer grows by a shift of its phase boundary towards the Si phase. Similarly, Y and Cu are not involved in a long-range diffusion since the Y–Cu–O layer must grow at its phase boundary into the Y123 phase after the depletion of Y123 from Ba and O. This interrelated reaction diffusion would be impeded by the formation of a gap if there are not enough point contacts between Si and $BaSiO_3$ and, eventually, the reaction may cease.

An initial stage of the reaction was observed in a sample annealed at 700 °C/20 h. Directly after cutting, without further metallographic preparation, the Si wafer was separated from the Y123 tablet and the reacted surface of the tablet was studied by SIMS. The compositional depth profile is given in Fig. 7 and an enrichment of Ba and Si in the surface region is clearly visible. An unreacted Y123 tablet, analysed for comparison, did not show this segregation. This finding is consistent with the barium silicate formation initiating the reaction, as discussed above with Fig. 6.

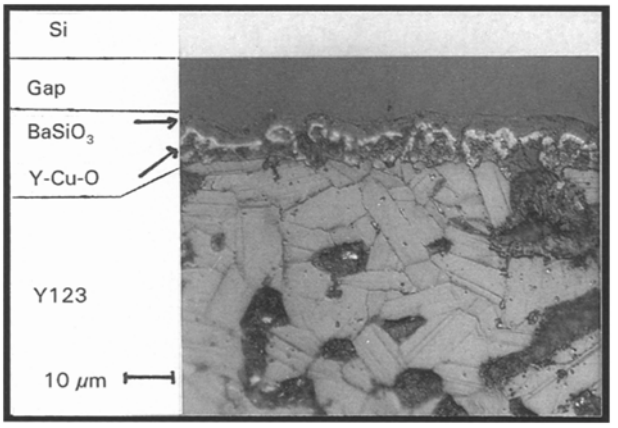

Figure 5 Cross-sectioned reaction zone of a Si/Y123 couple after 20 h at 800 °C (optical micrograph). $BaSiO_3$ was occasionally mixed with Ba_2SiO_4.

TABLE VI Growth of reaction zone R with total thickness d at various annealing temperatures and times in quasi-infinite Si/R/Y123 diffusion couples

	5 h		20 h		80 h	
T (°C)	R	d (μm)	R	d (μm)	R	d (μm)
650 °C	none	–	none	–	none	–
700 °C	none	–	(Ba + Si)[a]	–	$BaSiO_3$/ Y–Cu–O[b,c]	5
750 °C	none	–	$BaSiO_3$/ Y–Cu–O[b,c]	10	$BaSiO_3$/ Y–Cu–O[b,c]	12

none = no reaction zone observed (SEM/EDX, WDX).
[a] Ba + Si enrichment at Y123 surface (SIMS).
[b] In addition to $BaSiO_3$ some Ba_2SiO_4 was also found.
[c] Y–Cu–O is probably multiphase Y_2O_3 + Cu + Cu_2O.

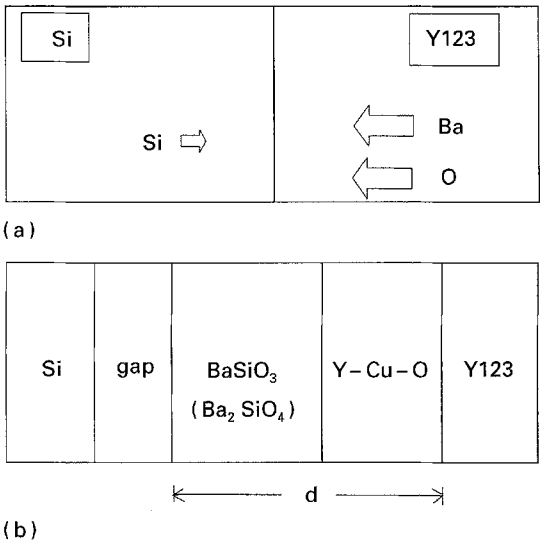

Figure 6 Schematic diagram of a cross-sectioned Si/Y123 couple: (a) major species, diffusing through reaction zone; (b) growing phase sequence in the reaction zone R.

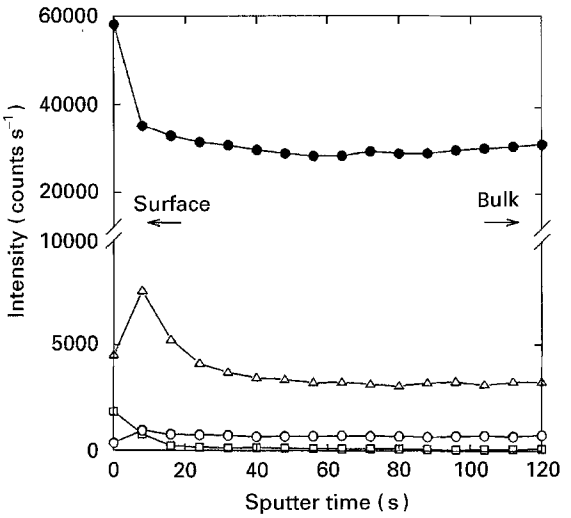

Figure 7 SIMS depth profile from a Y123 sample after contact with a Si wafer for 20 h at 700 °C. ● Ba; △ Si; □ Cu; ○ Y.

At an even earlier reaction stage the formation of SiO_2 was observed in the thin film experiments of Li and Williams [1]. This SiO_2 layer obviously serves as a diffusion barrier at lower temperatures up to ~100 °C. Upon annealing at 200–300 °C, after

most of the initial 3 nm Si film was oxidized, the segregation of Ba to the top of the film was observed. This was explained by the more likely diffusion of Ba through an SiO_2 film as compared to a Si film.

It may be suggested from our present data that a barium silicate had formed on top of the film. This would correspond to a final stage of the reaction depicted in Fig. 6 after all the Si is reacted, leaving a $BaSiO_3$ layer on top. This formation of a stable double oxide would also explain the observed [1] decrease of SiO_2 features in the AES spectrum of an SiO_2 film deposited and annealed on Y123.

3.2.2. Bulk samples Y123+Si

The bulk mixtures of Y123 powder with Si (powder and pieces) annealed at 800 °C for 100 h all exhibited the same phases according to the XRD data as follows: Si, Cu, $BaSiO_3$, Ba_2SiO_4, Y_2O_3. No change is observed after an additional annealing for 100 h. These phases were found for all mass ratios (Y123:Si = 2:1, 4:1, 10:1), with the Si intensities decreasing in this sequence. In the sample with the highest Y123 content (mass ratio = 15.68:1) additional traces of Cu_2O were found.

From a comparison of a number of potential reaction products and their thermodynamic data [10] the following primary reaction may proceed:

$$2YBa_2Cu_3O_{6.5} + 3Si \rightarrow 2BaSiO_3 + Ba_2SiO_4 + Y_2O_3 + 6Cu \quad (3)$$

The Gibbs energy of this reaction, using the data in Table V, is given by

$$\Delta G_{(3)}(1100\,K) \approx -2195.9\,kJ\,mol^{-1} = -78.5\,kJ\,g\text{-}atom^{-1} \quad (4)$$

The stoichiometric proportions of Equation 3 correspond to the sample with the mass ratio (15.68:1) and all of the product phases were actually found. The additional traces of Cu_2O are a result of a slight oxygen excess since the Y123 tablets are prepared with $O_{6.8}$ instead of $O_{6.5}$. The four reactant phases of Equation 3 together with Cu_2O form a non-variant equilibrium of five condensed phases at 800 °C which also fixes the oxygen partial pressure, probably very close to the value of the binary Cu/Cu_2O equilibrium.

For all the understoichiometric samples with mass ratios below (15.68:1) an excess of the unreacted Si phase is expected from Equation 3 and was actually found. This presence of substantial amounts of pure Si explains the absence of Cu_2O in these samples, since Cu_2O would be easily reduced by Si.

3.3. Tungsten silicide

Cross-sections of the WSi_2/Y123 diffusion couples could not be prepared metallographically since the WSi_2 powder did not sinter and the samples disintegrate during handling after annealing. A hard core – the former Y123 tablet – could be isolated from most samples and was studied using SEM/EDX. It consists of Y–Cu oxides, indicating that the small Y123 tablet of the diffusion couple was completely reacted after 100 h at 800 °C. The surrounding powder of this sample was studied by XRD and consists of various Ba compounds as given in Table VII.

TABLE VII Results of bulk samples (Y123 + WSi_2) annealed at 800 °C for 100–200 h

Mass ratio (Y123:WSi_2)	Phases identified (sequence according to X-ray intensities)
10:1	$Cu_2O + YCuO_2 + BaSiO_3 + BaY_2O_4 + BaWO_4 + Cu + \cdots$
5:1	$BaWO_4 + Cu + Y_2O_3 + Ba_2CuWO_6 + Ba_2CuO_3 + BaSiO_3 + BaY_2O_4 + \cdots$
3.5:1[a]	$WSi_2 + BaWO_4 + BaSiO_3 + Ba_2Y_{0.667}WO_6 + \cdots$
2:1	$WSi_2 + BaWO_4 + BaSiO_3 + Ba_2CuWO_6 + \cdots$

[a] Diffusion couple, completely reacted after 100 h and isolated from the Y–Cu–O core.

The XRD analysis of the bulk powder mixtures, also given in Table VII, was much more difficult. The XRD spectra are very complicated since they also comprise all the Y–Cu–O phases intermixed in the samples of this six-component system. However, the five major peaks of each of the phases given in Table VII could be unequivocally identified. A reaction equation cannot be given based on these data.

The main result of our experiments with WSi_2 is that its chemical reactivity with Y123 is not much smaller than for the elemental components, W and Si. One reason may be that the chemical stability of WSi_2 is not very large if we compare its Gibbs energy of formation on the basis of 1 mole of atoms ($\Delta_f G = -28\,kJ\,g\text{-}atom^{-1}$) to that of the other compounds in this system (see Table V). There are no additional compounds containing both W and Si among the reaction products compiled in Table VII. New phases observed are $YCuO_2$, BaY_2O_4, Ba_2CuWO_6 and Ba_2CuO_3. Most of the products in Table VII are higher Ba-oxides which also formed in the experiments with elemental W and Si.

It is concluded from the experimental evidence that the low thermodynamic stability of Y123, compared to the Ba compounds, in conjunction with the fast diffusion of barium through the forming reaction products are mainly responsible for the high reactivity of Y123 with WSi_2, W and Si.

3.4. Comparison of reactions in bulk samples and diffusion couples

A major result is that the reactions in bulk mixtures and diffusion couples are consistent and complement each other. For tungsten, the dominating product, $BaWO_4$ (Table III), is also found in the diffusion couple (Fig. 3). The fine grained Y–Cu–O layer is easier to analyse using XRD and the phases observed after the consumption of Y123, mostly Y_2O_3 + Cu,

are given in Table III. On the other hand, the WO_z layer, with the variation of z, is easier to resolve in the diffusion couple since it is distributed over a large space adjacent to the residual reservoir of W.

The same consistency applies in the case of silicon, where a smaller number of phases develops and the relationship between Fig. 6 and Equation 3 is even more clear.

The phases observed in both types of experiments will not be completely identical since the phase formation along the diffusion path in a quasi-infinite diffusion couple is governed by the local equilibria while in the bulk sample an overall equilibrium may be established among the reaction products on the right-hand side of Equations 1 and 3. However, the dominant products are often also encountered along the diffusion path and this is in fact the case for the present material combinations.

It is to be noted that the reaction kinetics at 800 °C in bulk samples are faster for Si (complete reaction after 100 h) compared to W (partially incomplete reaction after 200 h). This is further indication that the seemingly faster growing reaction zone in W/Y123 couples (50 μm after 80 h) compared to Si/Y123 (12 μm after 80 h) is an artefact, caused by the poor mechanical contact between the Si wafer and the Y123 tablet.

4. Conclusions

1. The superconductor Y123 is not in thermodynamic equilibrium with W or Si or WSi_2. Large thermodynamic driving forces can be quantitatively given for W and Si and the dominant reaction products are found in bulk powder mixtures as well as in quasi-infinite diffusion couples.

2. The reactivity of WSi_2 is not much smaller compared to that of elemental W and Si.

3. The diffusion through the reaction zone, and not in the initial contact phases of the diffusion couple, dominates the process. A theoretical approach based on diffusion coefficients of all species in all phases will be difficult. An overall diffusion-controlled mechanism could be verified for the W/Y123 couple.

4. Similarities are observed for W/Y123 and Si/Y123: barium, and also oxygen, are dominantly diffusing species in all cases. Barium moves far through the reaction zone to form double oxides, leaving a fine grained Y–Cu–O layer behind (mostly Y_2O_3 + Cu) and eventually the entire superconductor phase Y123, being depleted of Ba, turns into this Y–Cu–O mixture. At a later stage the pure W, Si or WSi_2 will be completely consumed, unless they were added in excessive amounts.

Acknowledgements

This project has been supported by the Bundesminister für Forschung und Technologie (BMFT) under grant No. 13N5702. The responsibility for the technical content is with the authors. Thanks are due to J. Claus (TU Clausthal) for the SIMS measurement of the Si/Y123 sample and to M. Schubert (TU Braunschweig) for the resistivity measurements.

References

1. BIN LI and E. D. WILIAMS, *J. Mater. Res.* **6** (1991) 1634.
2. D. M. HILL, H. M. MEYER III, J.H. WEAVER and N. D. SPENCER, *Surf. Sci.* **236** (1990) 377.
3. P. KULKARNI, S. MAHAMUNI, M. CHANDRACHOOD, I. S. MULLA, A. P. B. SINHA, A. S. NIGAVEKAR and S. K. KULKARNI, *J. Appl. Phys.* **67** (1990) 3438.
4. H. KOINUMA, K. FUKUDA, T. HASHIMOTO and K. FUEKI, *Jpn. J. Appl. Phys.* **L27** (1988) L1216.
5. BOKHIMI, *Physica C* **175**(1991) 119.
6. A. GARCIA-RUIZ, BOKHIMI and M. PORTILLA, *J. Mater. Res.* **7** (1992) 24.
7. N. CHEN, S. J. ROTHMANN and J. L. ROUTBORT, *Ibid.* **7** (1992) 2308.
8. W. WOONG-NG, H. MCMURDIE, B. PARETZKIN, C. HUBBARD and A. DRAGOO, JCPDS Graint-in-Aid Report, JCPDS card no. 39-486 (1987).
9. R. BOHNENKAMP-WEIß, Dr. -Ing. thesis, TU Clausthal (1993).
10. I. BARIN, "Thermochemical data of pure substances", 2nd edn (VCH, Weinheim, 1993).
11. T. MATHEWS and K. T. JACOB, *Metall. Trans. A* **23A** (1992) 3325.
12. P. VILLARS and L. D. CALVERT, "Pearson's handbook of crystallographic data for intermetallic phases", 2nd edn (American Society for Metals, 1991).

Received 3 December 1993
and accepted 3 February 1995